

## Upper Limits on Cross Sections for $\gamma + n \rightarrow K^0 + \Lambda^0(\Sigma^0)$ below 1500 MeV\*†

DONALD G. COYNE‡

AND

JOE H. MULLINS

*California Institute of Technology, Pasadena, California*

(Received 23 November 1966)

A search for the reactions  $\gamma + n \rightarrow K^0 + \Lambda$  and  $\gamma + n \rightarrow K^0 + \Sigma^0$  has been conducted using the Cal Tech heavy-liquid bubble chamber as the detector with a central internal target. Photon energies were from threshold to 1530 MeV. The absence of any real events in 14 000 pictures implies a joint upper limit on the average total cross sections  $\bar{\sigma}_\Lambda$  and  $\bar{\sigma}_\Sigma$  in this energy region. If the ratio  $\bar{\sigma}_\Lambda/\bar{\sigma}_\Sigma$  is near unity, we find at the 90% confidence level:  $\bar{\sigma}_\Lambda \leq 2.4 \mu\text{b}$ ,  $\bar{\sigma}_\Sigma \leq 2.1 \mu\text{b}$ .

### I. INTRODUCTION

THE associated photoproduction reaction  $\gamma + p \rightarrow K^+ + \Lambda$  may be studied by standard counter-spectrometer techniques, and detailed information is currently being amassed on excitation functions, differential cross sections, and polarization of the  $\Lambda$ .<sup>1-4</sup> Some data also exist on the reaction  $\gamma + n \rightarrow \Sigma^- + K$ .<sup>5</sup> Extension of the experimental study to

$$\gamma + n \rightarrow K^0 + \Lambda^0,$$

$$\gamma + n \rightarrow K^0 + \Sigma^0$$

is difficult because the neutrals may be detected only after decay, i.e., in a multiparticle final state ( $\pi^+\pi^-\pi^-\rho$  or  $\pi^+\pi^-\pi^-\rho e^+e^-$ , respectively). Multiple  $\pi$  photoproduction is then a very competitive background for counter or triggered spark-chamber techniques. We have used a bubble-chamber technique to search for this reaction, primarily to determine if the (unknown) total cross sections are large enough to make further study of these reactions statistically fruitful. The underlying motivation for leaving the charged mode for a more experimentally demanding reaction is that the theoretical analysis of the neutral mode is simpler, and details of the  $K$ -hyperon interaction are more subject to phenomenological investigation.

Our technique was expected to yield only about 5 counts for the combined reactions for a small sample of pictures, and the observed occurrence of *no valid counts* allows us to set upper limits on the combined neutral

cross sections. This paper is in the spirit of suggesting to future experimenters a reasonable maximum count rate to be expected. Discussion of a few of the comments above, and justification of our confidence in the null result, follows in Secs. II, III, and IV. A quantitative presentation of the upper limits is given in Sec. V.

### II. MOTIVATION

The Feynman diagrams shown in Fig. 1 might be hoped to adequately describe all associated photoproduction reactions (the open circles represent a choice of interaction with charge or anomalous magnetic moment). The  $P_{1/2}$  resonance in the direct term (a) is one possible "cause" of the observed bump in

$$\pi^- + p \rightarrow K^0 + \Lambda^0$$

near  $E_{\text{c.m.}} = 1700$ , but usually the  $N_{1/2}^*(1688)$  is credited as being the source of the bump. The situation is not entirely clear in the strong interaction,<sup>6</sup> and the charged associated photoproduction data does not clarify the situation.<sup>7</sup> Models using various combinations of the above terms do not fit all existing data simultaneously.<sup>3,8</sup> The expected effects of the  $N_{1/2}^*$  ( $A$  or  $F$  state) do not appear in the angular distributions.<sup>1,3</sup>

Since the claim is made<sup>9</sup> that the term (b), with  $K^+$ , contributes to all partial waves in a way which may mask the effects of a  $N_{1/2}^*$  intermediate state, it is natural to want the comparable data from the neutral mode where this term is absent. Furthermore, the pre-

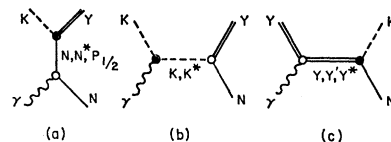


FIG. 1. Feynman diagrams for  $\gamma + N \rightarrow K + Y$ .

\* Work supported in part by the U. S. Atomic Energy Commission. Prepared under Contract No. AT(11-1)-68 for the San Francisco Operations Office, U. S. Atomic Energy Commission.

† Based in part on work submitted to the California Institute of Technology in partial fulfillment of the requirements for the degree of Doctor of Philosophy. (D.G.C.)

‡ Present address: Lawrence Radiation Laboratory, University of California, Berkeley, California.

<sup>1</sup> A. J. Sadoff, R. L. Anderson, E. Gabathuler, and D. Jones, *Bull. Am. Phys. Soc.* **9**, 34 (1964).

<sup>2</sup> H. Thom *et al.*, *Phys. Rev. Letters* **11**, 433 (1964).

<sup>3</sup> C. W. Peck, *Phys. Rev.* **135**, B830 (1964).

<sup>4</sup> D. E. Groom, Ph.D. thesis, California Institute of Technology, 1965 (unpublished).

<sup>5</sup> R. L. Anderson, F. Turkot, and W. M. Woodward, *Phys. Rev.* **123**, 1003, (1961).

<sup>6</sup> G. T. Hoff, *Phys. Rev. Letters* **12**, 652 (1964).

<sup>7</sup> For a more recent analysis of the  $K^+\Lambda$  photoproduction data, see H. Thom, *Phys. Rev.* **151**, 1322 (1966).

<sup>8</sup> C. W. Peck, Ph.D. thesis, California Institute of Technology, 1964 (unpublished).

<sup>9</sup> M. Gourdin and J. Dufour, *Nuovo Cimento* **27**, 1410 (1963).

dictions for the cross sections of the neutral modes tend to be comparable or larger than the charged modes, both from the above models<sup>10</sup> and from symmetry theories.<sup>11</sup> Experimentally, the only prior number for the neutral cross sections is from a subtraction of two statistically uncertain results,<sup>12,13</sup> giving

$$\bar{\sigma}_{\Lambda K^0} = \bar{\sigma}_{\Sigma^0 K^0} = 4 \pm 3 \mu\text{b}$$

(averaged over photon energies from threshold to 1350 MeV).

Our experiment was designed only to check more directly the above number and to see if the extrapolation of the models is justified (they all fit many parameters to existing data to get even their partial agreement).

### III. TECHNIQUE

The detector in this experiment was the Cal Tech 12-in. heavy-liquid bubble chamber, operated with a central beam tube containing high-pressure D<sub>2</sub> gas. The chamber has no magnetic field, since containment of the shower due to the high intensity beam ( $3 \times 10^5$  equivalent quanta/picture) is absolutely necessary. The dense liquid (CF<sub>3</sub>Br) serves mainly as an analyzer, using known range-energy and multiple-scattering relations. Our configuration was necessitated by the desire to have a large number of interactions in a small number of pictures.

An exposure of 50 000 pictures was made using the Cal Tech Electron Synchrotron with electron energy of 1530 MeV. The photon beam generated by letting such electrons strike the internal tantalum target was collimated to 0.022 in. diam, "hardened" (photons < 10 MeV removed) by lithium hydride in a pulsed field, recollimated to 0.032 in. fed into a vacuum tube and swept by 6.5 kG m of field to remove non-neutral components, peripherally scraped by a lead collimator, and finally introduced through a Mylar window into the deuterium gas target. This sequence is shown in Fig. 2, which shows all important features of the experimental layout.

Alignment of this system was first accomplished by x-ray photography to pass beam through the system, with final lineup being done by maximization of flux through each element, using an ion chamber as the quantitative element. All collimators were alignable with micrometer accuracy (0.002 in.). A compromise between premature beam dump and vertical blow up of the beam fixed both the synchrotron fundamental frequency and the radiator position. The chamber itself was aligned by a sequence of x-ray pictures allowing the

chamber beam tube to be accurately (0.003 in.) centered around the pre-aligned pencil beam.

Monitoring of the beam intensity was carried out by a counter telescope system due to L. J. Fretwell and J. H. Mullins. This telescope, viewing particles created by the photon beam hitting a polyethylene target as it exited from the bubble chamber, is necessary because saturation (of an otherwise indeterminable amount) takes place in ordinary ion chambers and quantimeters when used with the intense, fast-dumped beam necessary for the bubble chamber. The counter system was continuously cross-calibrated with an ion chamber by using at least two slow beam dumps between each fast dump intended for a bubble-chamber exposure. The typical beam intensity monitored was a total integrated energy of  $5 \times 10^9$  MeV of photons dumped in 100  $\mu\text{sec}$ . This total flux is but a tiny fraction (0.00001) of the original energy of the electrons in the synchrotron. The extensive neutron,  $\gamma$ , and charged-particle shielding shown in Fig. 2 was to deal with the chamber-obscuring background, both beamline associated and from general room sources, caused by the dissipation of essentially all of the original energy of the electrons.

About 14 000 of the pictures were then scanned by at least four different people, who looked for *single* vees originating in a fiducial volume, and which satisfied geometrical tests based on the possible kinematics of true events. The total pool of single vees was then processed to produce all candidates with the characteristic double-vee signature of  $K^0\Lambda$  or  $K^0\Sigma^0$  (no attempt was made to see a converting  $\gamma$  from  $\Sigma^0$  decay because of high electron background). Geometrical tests based on the possible kinematic correlations of these two vees were then applied. Surviving candidates were then measured and kinematically fitted, using a maximum-likelihood technique and the nonlinear variable metric minimization routine MIN.<sup>14</sup> The fitting program was devised especially for the  $K^0\Lambda$  reaction, which is twice overdetermined by only the angles of the final-state particles (if all masses are known). The reaction is further overconstrained by multiple spatial measurements and *a priori* knowledge of the beamline and the deuteron wave function. Selection criteria for real events (see Sec. IV) were then imposed on the distributions of  $\chi^2$  and various other physical parameters.

The bubble-chamber configuration used here is not recommended if it is possible to use a low-flux beam at a remote location of the chamber from the synchrotron, and then to eliminate the beam tube and apply a magnetic field. The choice is between moderate numbers of very "busy" pictures and large numbers of easily scannable pictures. The latter now looks preferable if at all possible.

<sup>10</sup> See, e.g., Fayyazuddin, Phys. Rev. **134**, B182 (1964).

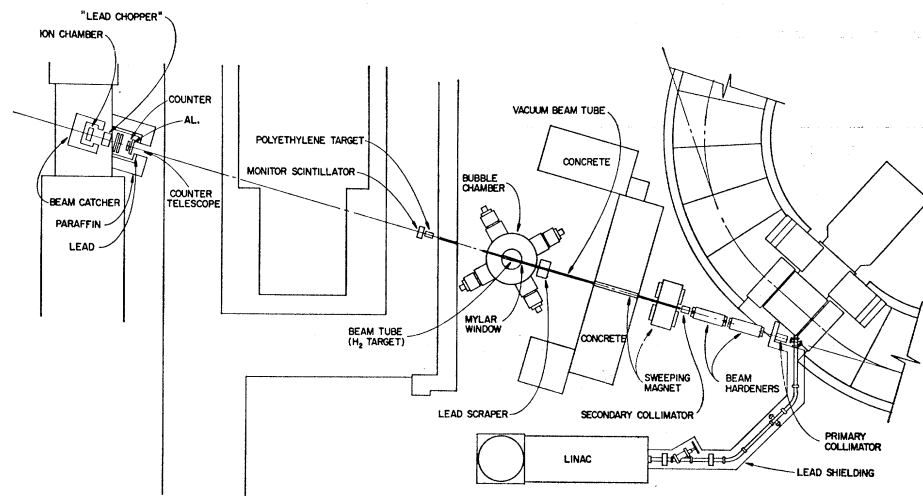
<sup>11</sup> L. Holloway and A. Fujii, Nuovo Cimento **28**, 1517 (1963).

<sup>12</sup> E. D. Alyea, Ph.D. thesis, California Institute of Technology, 1962 (unpublished).

<sup>13</sup> A. D. McInturff and C. E. Roos, Phys. Rev. Letters **13**, 246 (1962); and private communication.

<sup>14</sup> W. C. Davidon, Argonne National Laboratory Report No. ANL-5990 Review (1959) (unpublished).

FIG. 2. Experimental arrangement and beam area.



#### IV. JUSTIFICATION OF SCREENING TESTS

The primary suspicion in a low-count-rate experiment is that either real events were missed because they have a characteristic low scanning efficiency, or that they are eliminated by some screening test (at the table or in the computer). An elaborate Monte Carlo calculation was made to simulate events and their measurement with high integrity. This involved generation of events with all degrees of freedom actually present, including human error. The latter was simulated by outputting computer-drawn pictures of bubbles making up tracks, complete with multiple scattering, stereo simulation, proper spatial distributions, and range relations, so that the normal steps involving human error could be carried out by the usual staff. These simulated events were used to evaluate the efficiencies of both geometrical and kinematic fitting screening tests, as well as to prove that the real events would be extremely unlikely to fall into classes with below average scanning efficiencies.

Using the "expected" excitation functions shown in Fig. 3 (from a calculation of Kawaguchi and

Moravcsik<sup>15</sup>) and flat c.m. angular distributions (the result turns out not to be very sensitive to these assumptions), the expected loss of real events because of various

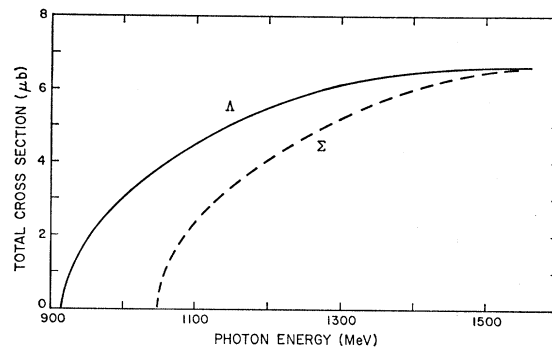


FIG. 3. Nominal theoretical cross sections.

screening tests is given in Tables I and II. Also given is the background/foreground ratio after each test, with foreground predicated on the same curves of Fig. 3. It is

TABLE I. Purification of sample at scanning table.

Test	% loss of real events (given by Monte Carlo calculation)	Background/foreground (using predicted number of counts) after test at left:
All possible 2-vee combinations	(Limited by scanning efficiency)	45 000
Large opening angles	<0.1%	7 200
Unreal origins	negligible	4 200
Fiducial volume ( $y_0$ )	<0.1%	2 500
Electron pairs	negligible	1 600
$2\nu$ same side	$1 \pm 1\%$ ( $K\Sigma$ only)	710
$2\nu$ origins incompatible	negligible	530
Coplanarity of $KY\gamma$	negligible	430
Backward-going neutrals	$0 \pm 0.1\%$	320
Improbable decay angles	$0 \pm 0.5\%$	107
Improbable decay vertices	$0.8 \pm 1\%$	100

<sup>15</sup> M. Kawaguchi and M. J. Moravcsik, Phys. Rev. **107**, 563 (1957).

TABLE II. Purification of sample by kinematic fitting.

Requirement	Surviving fraction of initial No. of events		Background/foreground (using predicted number of counts)
	$K\Lambda$	$K\Sigma^0$	
$\chi^2 \leq 100$	98.5 ± 1%	98.5 ± 1%	43
Origin, $\gamma$ -energy physical	96.5 ± 1.4%	93.6 ± 2.2%	9
$\chi^2/N \leq 2.25$	94.6 ± 1.7%	88.9 ± 3.0%	1.8
[Include pre-analysis scanner tests]	93.7 ± 2.5%	87.0 ± 3.5%	1.8
Neutron momentum $\leq 200$ MeV/c	87.6 ± 3.6%	82.4 ± 7.1%	0.4
Particle identification	73.1 ± 4.0%	68.9 ± 8%	0

seen that the remarkable attenuation of this ratio comes from the application of very conservative tests which do not result in appreciable losses of real events.

V. RESULTS

In the interest of brevity, we present only one of several similar distributions which compare the analysis system acting on generated events to the same system acting on the true data. Figure 4 shows the expected

distribution (generated events) of  $\chi^2/N$ , with  $N$  the number of degrees of freedom for a particular fit (ranges from 5 to 15). Note that the two reactions are both well fitted by the kinematics of  $K\Lambda$ : The reactions cannot be separated in this experiment. As listed in Table II, a cutoff at  $\chi^2/N < 2.25$  retains about 92% of all real events. The data, with no additional tests imposed, show no evidence of any peaking near  $\chi^2/N \simeq 0.75$ , as is shown in Fig. 5. If all the physical requirements listed

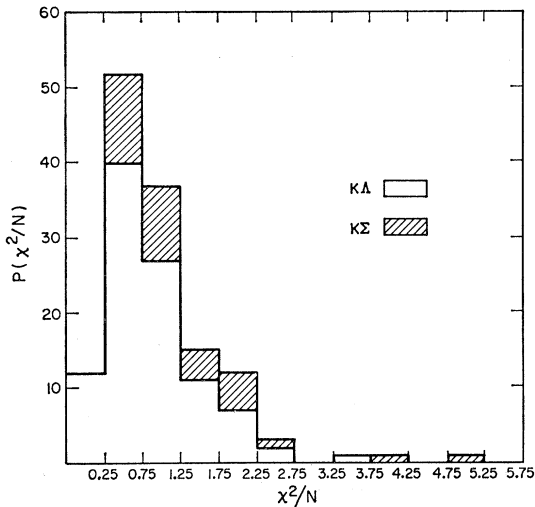


FIG. 4. Distribution of ( $\chi^2$ /degrees of freedom) for Monte Carlo generated events.

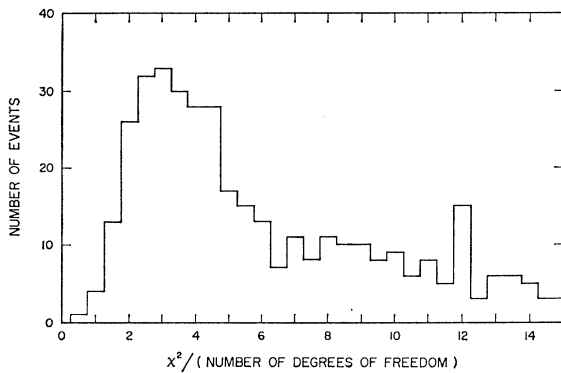


FIG. 5.  $\chi^2/N$  distribution of the data (no restrictions).

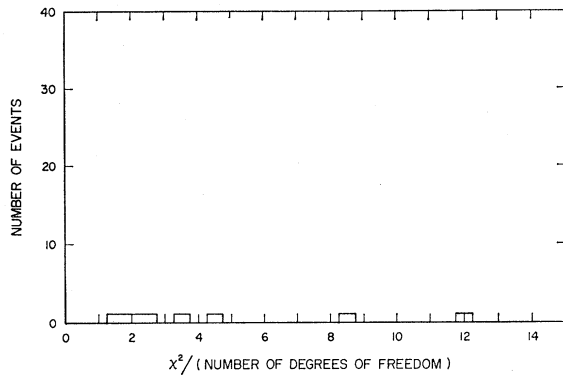


FIG. 6.  $\chi^2/N$  distribution of the data (all restrictions).

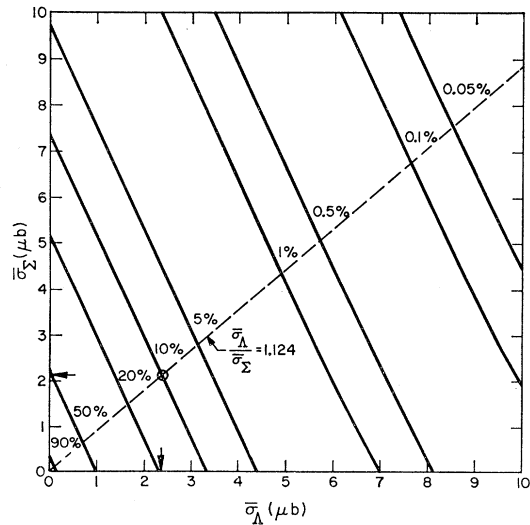


FIG. 7. The probability that no events are seen if true cross sections are  $\bar{\sigma}_\Lambda$  and  $\bar{\sigma}_\Sigma$ .

in Table II, except for particle identification, are imposed, the background (highly unphysical) disappears and the remaining events appear as shown in Fig. 6. These events have particle identification incompatible with real  $K\Lambda$  decays. A previous experiment<sup>16</sup> with similar pictures showed that only 3.7% of all true events would have particle-identification errors of this sort: a particle unequivocally called a pion which is really a proton. Furthermore, multiple remeasurements of the events are all rejected (background events tend to have shallow minima in the log of their likelihood functions, and are usually widely changed upon remeasurement), and these "marginal" events have physical features, like long lifetimes, placing them below 0.1% probability of being real. Thus the most probable conclusion of this experiment is that no real events were seen.

In Fig. 7, we show a contour map of the probability of this result as a function of the total cross sections (averaged from threshold to 1530 MeV) of the  $K\Lambda$

<sup>16</sup> L. J. Fretwell, Jr. and J. H. Mullins, Phys. Rev. 155, 1497 (1967).

and  $K\Sigma$  reactions,  $\bar{\sigma}_\Lambda/\bar{\sigma}_\Sigma$  as given by the behavior in Fig. 3. For this ratio only, we use the 10% contour (corresponds roughly to the 90% confidence level) and find the upper limits

$$\begin{aligned}\bar{\sigma}_\Lambda &\leq 2.4 \mu\text{b}, \\ \bar{\sigma}_\Sigma &\leq 2.1 \mu\text{b}.\end{aligned}$$

These upper limits indicate that previous estimates of these cross sections are too high. They certainly dictate a good deal of caution for the experimenter interested in obtaining a statistically significant sample of such events for phenomenological studies.

#### ACKNOWLEDGMENTS

We wish to thank our colleague, Dr. L. J. Fretwell, for ready exchange of information and techniques on parts of this experiment related to his work. We also acknowledge the help of the entire Cal Tech Synchrotron crew during the experimental run.

### Single and Multiple Pion Production in $\pi^+n$ and $\pi^-p$ Interactions at 1.7 GeV/c

T. C. BACON,\* W. J. FICKINGER,\* D. G. HILL, H. W. K. HOPKINS,\* D. K. ROBINSON,†  
AND E. O. SALANT\*

Brookhaven National Laboratory, Upton, New York

(Received 6 January 1967)

Meson production in  $\pi^-p$  and  $\pi^+n$  interactions at 1.7 GeV/c has been studied in two bubble-chamber exposures. Combined results are presented with emphasis on single-pion production (4300 events) which is dominated by the formation of the  $\rho^0$  meson in peripheral interactions, and on double-pion production (1100 events) which shows strong formation of the  $\omega$  meson. These data are compared with the predictions of particle-exchange models, including absorption, and the effects of competing channels are discussed. Evidence for a two-pion decay mode of the  $\omega$  is examined quantitatively. Processes with higher meson multiplicities are described.

#### I. INTRODUCTION

PION production in pion-nucleon interactions at 1.7 GeV/c has been studied in a bubble-chamber experiment. The following reactions have been analyzed and will be discussed in this paper:

- (1)  $\pi^- + p \rightarrow \pi^+ + \pi^- + n,$
- (2)  $\pi^+ + d \rightarrow \pi^+ + \pi^- + p + p_s,$
- (3)  $\pi^+ + d \rightarrow \pi^+ + \pi^- + \pi^0 + p + p_s,$
- (4)  $\pi^+ + d \rightarrow \pi^+ + \pi^- + \pi^+ + p + n,$
- (5)  $\pi^+ + d \rightarrow \pi^+ + \pi^- + \pi^+ + d,$
- (6)  $\pi^+ + d \rightarrow \pi^+ + \pi^- + \pi^+ + \pi^- + p + p_s,$
- (7)  $\pi^+ + d \rightarrow \pi^+ + \pi^- + \pi^+ + \pi^- + \pi^0 + p + p_s.$

Reactions (1) and (2), which are charge-symmetric, are dominated by  $\rho^0$  production, and reaction (3) by  $\omega$  production. The characteristics of the production and decay processes for these resonances will be discussed. Reactions (4) and (6) take place principally through production of the  $N^*(1238)$  isobar.

The symbol  $p_s$  in reactions (2), (3), (6), and (7) indicates that events were selected in which the pion interacted with the neutron in the deuteron, leaving a spectator proton.

#### II. THE EXPOSURES

The  $\pi^-p$  reactions were produced in the Brookhaven National Laboratory 20-in. hydrogen bubble chamber, exposed at the AGS to a negative beam of momentum 1.7 GeV/c. Since at this momentum the negative beam was almost entirely composed of pions, momentum

\* Present address: Vanderbilt University, Nashville, Tennessee.

† Present address: Western Reserve University, Cleveland, Ohio.